A Novel Approach for Performance-Based Design of Piles and Shafts under Liquefaction using Coupled Nonlinear Soil-Structure Interaction Analysis

Mohammad [Sasan] Iranpour, Ph.D., P.Eng.
Engineering Lead, Allnorth Consultant Limited, Vancouver, BC, Canada

ABSTRACT
One of the design challenges for bridges, buildings, port and marine structures is lateral spreading and ground liquefaction. There exist various simplified methods to study the behavior of structures in such soil conditions. However, in cases with large soil forces and movements, a plastic hinge may be generated in the structure, which adds to the complexity of the system. To avoid this, the general practice is to increase the capacity of the pile and shaft, which in turn increases the soil loads. In some cases, the soil loads increase at even a faster rate than the pile capacity, which ultimately makes it impossible to design a conventional structure based on the deterministic approaches provided by design standards.

Using the complex interaction of all stresses generated in the structure, this study presents a simplified approach based on a coupled nonlinear analysis of both the soil and the structure. It is demonstrated that when the pile enters the nonlinear range of the material response, it puts a limit on the loads that can be generated in the pile. This helps the designer move beyond the boundaries of traditional force-based design method, and use the more robust performance-based design approach, where a more accurate response of the system is taken into consideration.

RÉSUMÉ
L'épandage latéral et la liquéfaction des sols constituent l'un des défis de conception pour les ponts, les bâtiments, les structures portuaires et marines. Il existe différentes méthodes simplifiées pour étudier le comportement des structures dans de telles conditions de sol. Cependant, dans les cas où les forces et les mouvements du sol sont importants, une charnière en plastique peut être générée dans la structure, ce qui ajoute à la complexité du système. Pour éviter cela, la pratique générale consiste à augmenter la capacité du pieu et de l'arbre, ce qui augmente à son tour la charge du sol. Dans certains cas, les charges de sol augmentent même plus rapidement que la capacité du pieu, ce qui rend finalement impossible la conception d'une structure conventionnelle basée sur les approches déterministes fournies par les normes de conception.

En utilisant l'interaction complexe de toutes les contraintes générées dans la structure, cette étude présente une approche simplifiée basée sur une analyse couplée non linéaire du sol et de la structure. Il est démontré que lorsque le pieu entre dans la plage non linéaire de la réponse du matériau, il limite les charges pouvant être générées dans le pieu. Cela aide le concepteur à dépasser les limites de la méthode de conception traditionnelle basée sur les forces et à utiliser l'approche de conception basée sur les performances plus robuste, qui prend en compte une réponse plus précise du système.

1 INTRODUCTION

Many researches have been conducted recently to study the performance of structures under various loads. This has shaped the fundamentals of the performance-based design approach, which involves detailed modeling of the system and provides more extensive and accurate estimates of its response (Cassese et al. 2018). This level of information results in an improved evaluation of damages and losses, which helps the stakeholders to make more informed decisions. For cases where the structure is in direct interaction with soil, the evaluation of its performance can become complex, especially when the soil liquefies (Besseling 2012).

The engineering effort for a performance-based design can go considerably beyond what is normally used in contemporary practice; however, the benefits it provides are invaluable. Many believe that in the near future, performance-based design will be the normal standard for analysis and design of structures. This design approach can hardly be completed without a coupled nonlinear analysis and design of the system (Kramer et al. 2008; Iranpour 1999). For soil-structure interaction, this becomes even more significant due to the nonlinear soil properties and its complex interaction mechanism with the structure. In some cases, the structure also enters the nonlinear range of the material response. This changes the fundamental assumptions of the traditional soil-structure interaction analysis, and therefore, the analysis must be revised to capture these changes (Chandrakanth and Whittaker 2015).

This paper illustrates how shafts and piles in liquefiable soils can be designed to have a certain behavior during earthquake using a coupled soils-structure interaction analysis, where nonlinearities from both the soil and the structure are taken into consideration. While this study focuses on design of piles and shafts, it can be used for various structures such as bridges, buildings, tunnels, offshore and marine structures. This approach not only helps the engineers to finish the design based on specific performance requirements from the owner, but also to complete the design for cases where a traditional solution cannot be achieved using deterministic code approaches.

2 PERFORMANCE-BASED DESIGN

Performance-based earthquake engineering allows the owners and engineers to specify specific performance criteria for the structure based on its expected seismic response. This approach is used in many industries today, and accounts for different variables including ground motion, structural response, physical features, level of damage and other characteristics of the system. This level of information provides the knowledge required for a cost-effective management of resources for the design, evaluation, construction, monitoring and maintenance of structures and facilities. Many research programs have been completed to date to provide a better understanding of the performance of structures, and to develop more robust methodologies for performance-based design (Chandrakanth and Whittaker 2015; Kramer et al. 2008; Iranpour, 1999). Iranpour (1999) performed a detailed investigation into performance evaluation of concrete structures under various levels of seismic load, using a coupled nonlinear analysis and design approach (Iranpour 1999). That study demonstrated that some simplified approaches recommended by design codes and standards for evaluating the performance of the structure in the ultimate limit state were non-conservative, and resulted in considerable under-estimation of the response of the structure under earthquake. Further verified by other researchers (e.g. Miranda 2014; Krawinkler et al. 2012), such studies resulted in revisions to provisions of design standards, which now provide a better estimation of the response of the structure and its performance. This shows the importance and effectiveness of performance-based design, which can be implemented using different approaches such as coupled nonlinear analysis and design.

Performance-based design has been used by researchers for soil-structure interaction analysis and design with increasing success (Chandrakanth and Whittaker, 2015; Besseling, 2012 and Kramer et al. 2008). Depending on the soil layers and their characteristics, the piles and shafts embedded in soil will experience different responses. Figure 1 shows a schematic of piles and shafts in interaction with soil. In many cases (e.g. under liquefaction), a plastic hinge will be developed in the structure as it enters the nonlinear range of the material response. For shafts deformed in a single curvature, the location of the plastic hinge usually occurs at depth of 1.25 to 3.3 times the diameter of the shaft below the ground surface (Chai and Hutchinson 2002). For cases with double curvature, (see Figure 1), a more detailed analysis is needed to study the response of the structure under earthquake.

As shows in Figure 1, the soil profile studied in this research includes a layer that is susceptible to liquefaction under earthquake ground shaking. During liquefaction, the soil does not reach its ultimate resistance over the entire length of the pile. This results in large bending moment to be developed locally along a certain length of the structure. The location of the maximum bending moment depends on various factors including the soil profile, its characteristics, dimensions of the structure and its material properties. As the soil forces increase, the pile enters the nonlinear range of the material response, which creates a plastic hinge.

As explained later in this paper, the plastic hinge developed in the structure can be designed to have a certain response under earthquake loads using a coupled nonlinear analysis and design approach. This helps the engineer to implement a performance-based design approach to tune the overall response of the system to the performance requirements specified by the owner.

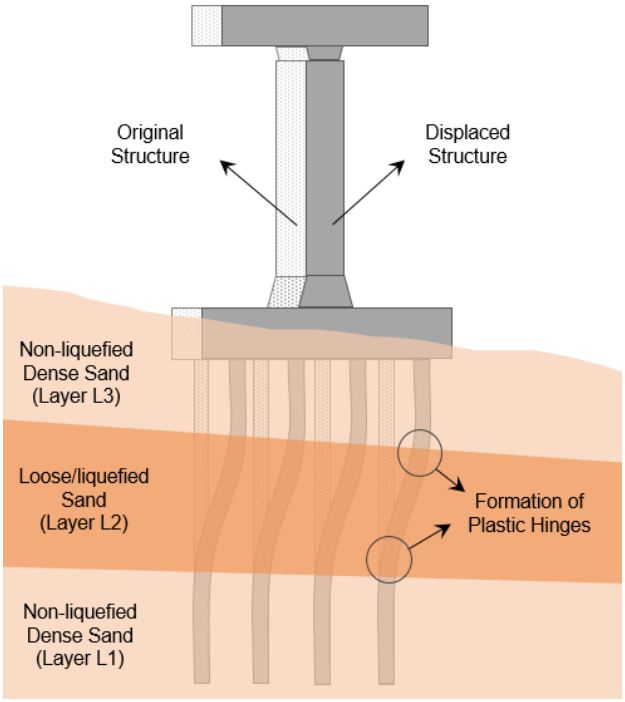

Figure 1. Schematic of Pile and Shaft Interaction with Different Soil Layers under Liquefaction during Earthquake

3 BEHAVIOR OF PILES AND SHAFTS DURING LATERAL SPREADING AND LIQUEFACTION

Many approaches have been developed to provide simplified solutions for engineers for a better estimation of soil-structure interaction. One of the approaches is the $p-y$ curve, where p is the soil resistance per unit length of the pile for a given pile deflection, y. The American Petroleum Institute (API) provides a widely used approach for calculating the $p-y$ curves. This approach implements the Matlock's approach for soft clay (Matlock, 1970) and the Reese's criteria for sand (Reese et at., 1974). The $p-y$ curves are calculated based on the bending moments capacity of the pile, using the governing equilibrium differential equation below:

$$p = \frac{d^2}{dz^2} M(z) \quad [1]$$

and, assuming a linear elastic bending moment for the pile, per:

$$\frac{d^2}{dz^2} \mathrm{y} = \frac{M(z)}{EI} \quad [2]$$

where p is the lateral resistance on the pile, y is the relative lateral pile displacement, M is the pile bending moment, EI is the flexural rigidity of the pile, and z is the vertical distance measured along the pile. As observed, the characteristics of the structure are taken into consideration by including the bending moment and flexural rigidity into the formulations. However, this approach does not directly consider the influence of shear and axial load, which can change the pile bending moment and flexural rigidity, especially in the nonlinear range of the material response.

Figure 2 shows the soil load and formation of cracks in a typical concrete pile or shaft. In additions to the $p-y$ curves that are used to calculate the lateral forces applied to the pile form the soil, there also exist $t-z$ and Q$-z$ curves that are used for calculating the vertical forces. The $t-z$ curves are used along the height of the shaft to calculate the downdrag soil forces in the vertical direction. The Q$-z$ curve is used at the very bottom of the pile to simulate the soil bearing pressure.

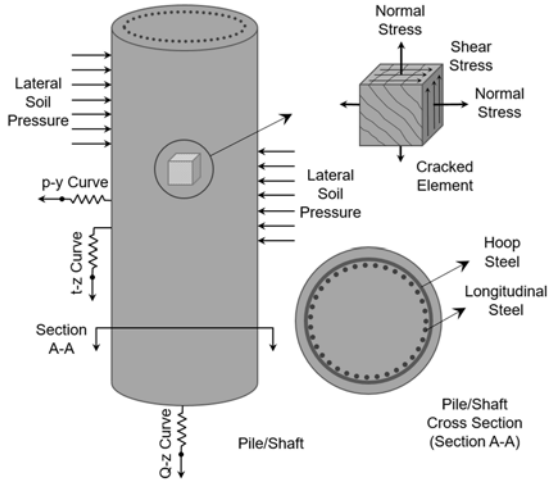

Figure 2. Soil Loads and Formation of Cracks in a Typical Reinforced Concrete Pile or Shaft

3.1 Static and Cyclic Loading

The conventional $p-y$ curves used for piles and shafts subject to monotonic and slow-rate cyclic loads are largely based on empirical test data. Researchers have demonstrated that the uncertainties in $p-y$ curve values could be overshadowed by assumptions of pile-head fixity in pile caps, choice of bending stiffness parameters for the piles, gapping effects, pile embedment effects and loading conditions (Lam et al. 1998). The $p-y$ curves developed for static and cyclic loadings are still used in many projects. However, for complex cases where the soil-structure interaction has a profound effect, the soil spring curves must include the effect of rapid loading and soil liquefaction explained in the next section.

3.2 Seismic Loading

Seismic loads are generated more rapidly in the soil, which results in excess porewater pressure built-up in the saturated soil layer. In such cases, the soil may liquefy, and the soil resistance may change due to the generation of porewater pressure. This, in turn, changes the forces applied to the structure from the soil.

There exist various methods for calculating the nonlinear $p-y$, $t-z$ and Q$-z$ soil springs for soil-structure interaction analysis: Wilson et al. 2000; Tokimatsu et al. 2001; Rollins et al. 2005 and Weaver et al. 2005. The soil spring curves in this research followed the study performed by Wilson et al. (2000), using the following soil properties:

Table 1. Soil Properties

Soil Layer (see Figure 1)	Layer 1	Layer 2	Layer 3
Water Content	25.7	35.6	32.6
Undrained Shear Strength (S_u, kPa)	450	100	N/A
Effective Friction Angle (degrees)	33	30	35
Permeability k_H k_V $(k, cm/sec)$	$10^{-6}-10^{-5}$ $10^{-7}-10^{-6}$	$10^{-6}-10^{-5}$ $10^{-7}-10^{-6}$	$10^{-4}-10^{-3}$ $10^{-5}-10^{-4}$

4 NONLINEAR COUPLED ANALYSIS AND DESIGN

Piles and shafts are under a complex set of loading combinations from soil. There exist various methodologies and approaches for detailed analysis of concrete structural members under combined loading conditions including axial, moment, shear and torsional forces. These include the Rotating-Angle Softened Truss Model RA-STM (Hsu 1993), the RA-STM 1995 (Belarbi and Hsu 1995), the RA-STM 1998 (Zhang and Hsu 1998), the Fixed Angle Softened Truss Model FA-STM 1996 (Pang and Hsu 1996), FA-STM 1997 (Hsu and Zhang 1997) and FA-STM (ASCE-ACI Committee 445 1998). One of the recent approaches for a comprehensive analysis and design of reinforced concrete structural sections is the Modified Compression Field Theory (MCFT), first developed by Vecchio and Collins in early 1980s (Vecchio and Collins 1986). This approach has been used extensively by many researchers and implemented in various programs for nonlinear analysis and design of concrete members (Bentz and Collins 2001; Bentz 2000). The next section briefly explains the fundamentals of the MCFT, followed by the structural analysis approach and derivation of the nonlinear interaction curves as implemented in this study.

4.1 Modified Compression Field Theory (MCFT)

Developed over 100 years ago, the original design procedure for reinforced concrete sections assumed that the cracked concrete in a beam resisted the shear stress

only by diagonal compressive stresses at an angle of 45 degrees to the longitudinal axis of the member. In reality, this angle is not constant and changes based on the stress condition of the cross section, which results in significant errors in the available traditional code-based design approaches. In the MCFT, this angle in calculated based on the longitudinal and transverse strain conditions of the cross section (Bentz et al. 2006). Verified by many experimental tests (Collins, et al. 2007; Bentz et al. 2006, Vecchio and Collins 1986), this theory demonstrated that even after extensive diagonal cracking, tensile stresses still existed in the concrete between the cracks. Combined with shear stresses on the crack faces, these tensile stresses have proved to increase the ability of the cracked concrete to resist shear (Bentz et al. 2006). This shows how the tensile stresses affect not only the shear capacity of the member, but also its bending moment capacity, as explained later in this study.

4.2 Detailed Nonlinear Analysis of the Cross Section

In this study, the stresses and strains for both the concrete and rebar were studied in detail for various cross sections with different loading combinations. The full load-deformation history of the elements was calculated based on the principals of the MCFT, using computer program Response 2000 (Bentz and Collins 2001). Various analysis result parameters were studies in details over the depth of the cross section, including longitudinal strain, transverse strain, shear strain/stress, principal compressive/tensile stress, crack diagram and shear on crack. Analysis results were used to create different interaction curves including moment-axial, moment-shear and axial-shear interactions.

For shear analysis, various plots were generated for shear stress versus shear-strain, as well as the moment curvature plot. This allowed for quick detection of shear failures versus flexural failures under different load conditions. The longitudinal strain plot were used to check the assumption that plane sections remain plane after bending. The longitudinal strains must be linearly distributed; however, the transverse strain depends on the local stress-strain conditions at each point across the cross section. The total vertical stress at every depth of the cross section must be equal to zero. The crack diagram was used to study the crack pattern, as well as crack widths along the length of the member. The crack spacing was calculated based on the angle and the estimate of crack spacing in the longitudinal and transverse directions as per the MCFT. The changes in the crack spacing over the depth of the cross section was also taken into consideration, which improved the analysis results.

The shear stresses were calculated for each incremental load level during the sectional analysis using the longitudinal stiffness of the cracked concrete. For cracked sections, the shear on the crack can maintain the principal tensile stress in the concrete. The principal compressive stresses were calculated and compared to the maximum allowable stress. The reduction of maximum allowable stress due to concrete cracking was calculated based on the principals of the MCFT. In some cases, the shear forces introduced diagonal compression, which resulted in principal compression over the entire depth of the cross section.

The principal tensile stresses were caused by the shear stresses acting on the cross section. The maximum allowable stress was calculated based on the requirements of longitudinal yield on the cross section. This helped understand if the section was approaching the flexural failure mode. The longitudinal reinforcement stress at a crack was used to study the effects of the shear on the crack and principal tension. The stirrup stresses were calculated as the average stress in the stirrups over the depth of the cross section. The stirrup stresses at crack ware calculated using equations of equilibrium, taking into account both the shear on the crack and principal tensile stresses.

4.3 Nonlinear Interaction Curves

The interaction curves in this study were developed using the procedure explained earlier. Figure 3 shows a typical axial-moment interaction curve developed in this study for a circular cross section reinforced concrete pile with a diameter of 1,000 mm and various percentage of longitudinal rebar. The cylinder strength of concrete is assumed to be 50 MPa at 28 days, with a tension strength and peak strain of 2.15 MPa and 2.25 mm/m, respectively. The rebar has a yield strength of 450 MPa and ultimate strength of 675 MPa. The strain hardening of both longitudinal and hoop steel is assumed to be 7 mm/m, with a rupture strain of 100 mm/m. The steel modulus of elasticity is 200 GPa. In this figure, positive axial force indicates tension, and negative axial force indicates compression on the cross section. Positive moment indicates compression on the top of the cross section.

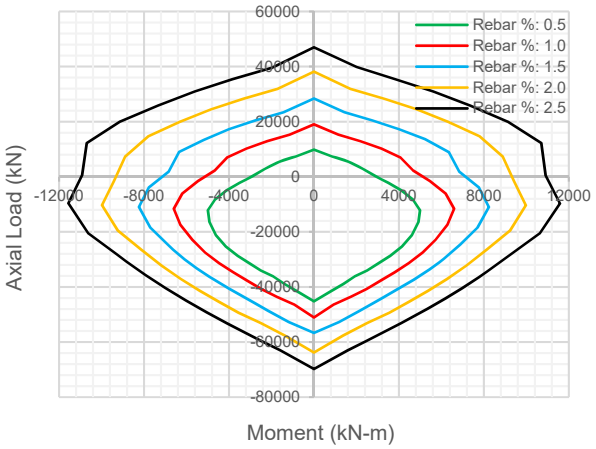

Figure 3. A Typical Axial-Moment Interaction Curve for Various Percentages of Longitudinal Steel Rebar

As observed in Figure 3, the interaction between the axial load and bending moment is nonlinear, especially at the upper limits of the bending moment capacity. The axial load is a function of different variables such as the dead weight of the structure, the ground water level and the downdrag from soil (in term of the nonlinear t$-z$ and $Q-z$ springs explained earlier). This results in significant

changes in the axial load acting on the cross section, which in turn, affects the maximum bending moment capacity of the cross section as illustrated in Figure 3. On the other side, there exist a nonlinear relationship between the bending moment and the curvature of the cross section. Under liquefaction and due to soil downdrag, the axial force changes, which results in changes in the bending moment of the cross section. This change in the bending moment results in changes in the curvature and deformation of the structure, which in turn results in changes in the soil lateral forces applied along the height of the structure captured by the $p-y$ curve approach. Moreover, the conventional $p-y$ curve approach does not consider the coupled interaction between the $p-y$ and t$-z$ curves, and therefore cannot capture all the soil continuum effect. This explains why a soil-structure interaction analysis does not only need to consider the nonlinear interaction between the soil and structure, but also need to take into account the nonlinear behavior of the structure itself, along with its influence on the soil-structure interaction.

Figure 4 shows a typical shear-moment interaction curve for the same circular cross section with various percentage of longitudinal rebar, and a hoop reinforcement of 10 M @ 250 mm on center. As shown in this figure, an increase in the longitudinal reinforcement from 0.5% to 1.0% slightly increases the maximum shear capacity of the cross section for a zero bending moment. However, any further increase in the percentage of the longitudinal steel does not increase the shear capacity of the member when no bending moment is applied to the cross section. In general, the percentage of longitudinal steel in shafts and piles is more than 1.0%. Therefore, it can be stated that for design purposes, an increase in the bending moment capacity (by increasing the percentage of longitudinal steel) does not result in an increase in the shear capacity of the member for low values of bending moment. However, as the bending moment increases and approaches the plastic hinge moment capacity, an increase in the longitudinal rebar significantly increases the shear capacity of the member.

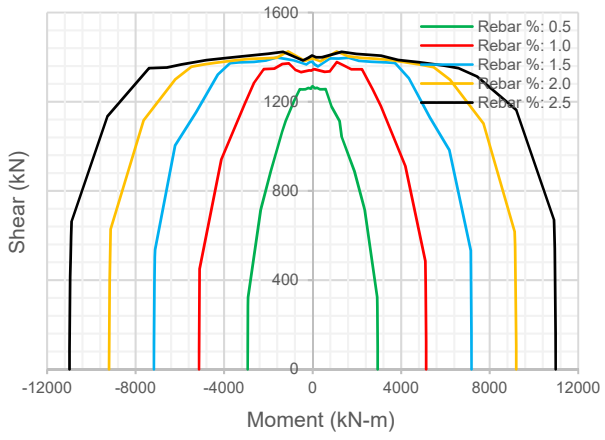

Figure 4. A Typical Moment-Shear Interaction Curve for Various Percentages of the Longitudinal Steel Rebar

Figure 5 shows a typical shear-axial load interaction curve for the same circular cross section with various percentage of longitudinal rebar. In this figure, positive axial force indicates tension, and negative axial force indicates compression on the cross section. Positive moment indicates compression on the top of the cross section. As illustrated in this figure, for axial compression up to about 40,000 kN, the shear capacity of the member is not a function of the percentage of the longitudinal steel rebar. Once the shear capacity reaches its maximum value, it abruptly drops to zero. This indicates a brittle shear failure, which is not desirable and must be avoided using a proper design philosophy and approach. Many researches have discussed in detail the importance of avoiding a brittle shear failure during the design of concrete structures (Cassese 2018; Qian et al. 2017).

The axial load in the pile and shaft can vary significantly during the seismic event and soil liquefaction. A linear uncoupled soil-structure interaction analysis for a constant level of axial load fails to represent the variation of the member capacity and ductility that occurs due to the fluctuation in the axial load. As observed in Figure 5, the section response and its ultimate capacity changes quite abruptly for higher levels of axial compression. This becomes even more important when a plastic hinge is developed in structure. Therefore, a nonlinear plastic hinge model which does not properly capture the complete interaction effect of all loads applied to the cross section will result in significant inaccuracy, especially for cases where axial load fluctuations control the capacity. This is another limitation of a soil-structure interaction analysis that does not take into account the nonlinearity from both the soil and the structure.

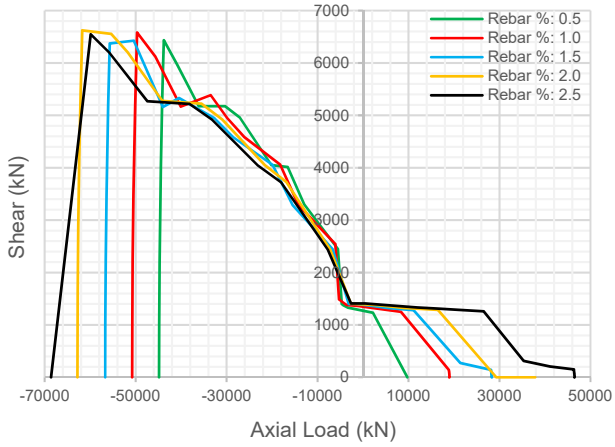

Figure 5. A Typical Shear-Axial Load Interaction Curve for Various Percentages of the Longitudinal Steel Rebar

Figure 6 shows a typical axial-moment interaction curve for various shear loads applied to the cross section with 1.5% of longitudinal steel rebar. As stated earlier, positive axial force indicates tension, and negative axial force indicated compression on the cross section. Positive moment indicates compression on the top of the cross section. As observed in this figure, the shear load does not reduce the axial compression load capacity of the member

as long as the member has not entered the nonlinear range of the material response. This is illustrated as the almost-linear portion at the lower portion of the interaction curves in Figure 6.

On the axial tension side of the graph in Figure 6, it is observed that application of a small shear load of 200 kN significantly reduces the axial tension load capacity of the cross section (by about 35% for zero bending moment). Further increase of the shear load up to 400 kN has very negligible influence (only 3% for a zero bending moment) on the axial tension load capacity of the cross section. Increasing the shear load on the cross section does not have any profound effect on further reduction of the axial load capacity, until it reaches a shear load of about 1,200 kN. This level is about 88% of the maximum shear load capacity of the section with no bending moment demand. When the shear load acting on the cross section reaches this limit, the axial tension load capacity of the cross section drops down to zero very rapidly.

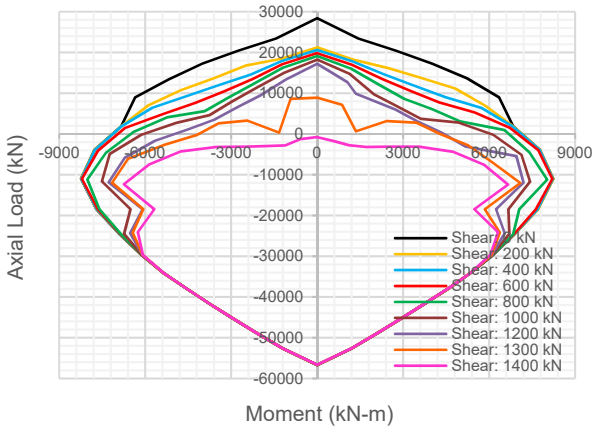

Figure 6. A Typical Axial-Moment Interaction Curve for Various Shear Loads Applied on the Cross Section with 1.5% of Longitudinal Steel Rebar

As illustrated in Figure 6, an increase in the shear load up to 600 kN (that is about 40% of maximum shear capacity of the cross section) does not have any influence on the ultimate bending moment capacity of the member. In other words, the creation of a moment plastic hinge in the cross section does not affect the shear resistance capacity of the member for lower shear demands. When the shear demand on the cross section exceeds 40% of its maximum shear capacity, the moment plastic hinge capacity starts decreasing. This, in return, decreases the soil load applied to the structure, as demonstrated earlier by equations 1 and 2. As shown in those equations, the load applied to the structure from the soil through the $p-y$ curve approach is a function of both the stiffness and bending moment of the structure.

When the structure enters the nonlinear range of the material response, it puts a maximum limit on the bending moment demand it can resist by limiting the maximum bending moment capacity to the plastic hinge moment capacity. As explained, this reduces both the bending moment and shear demand on the structure by decreasing the soil loads. This behavior can only be captured through a full nonlinear coupled soil-structure interaction analysis and design, where not only the soil nonlinearities, but also structural nonlinearities are taken into consideration. This is explained in details in the next section. Using this performance-based design approach, the engineer can design the system per the requirements specified by the owner.

4.4 Coupled Nonlinear Soil-Structure Interaction Analysis Results

The detailed cross section analysis and interaction curves developed earlier in this study were used as input for a coupled nonlinear soil-structure interaction analysis. Various 3D models were created in SAP2000 to study the influence of the nonlinear response of the structure, along with nonlinear behavior of soil using the $p-y$ curve approach.

At the start of the analysis, the cross section was assumed to have zero shear and bending moment demand, along with an axial load equal to the weight of the structure. During the analysis, the shear, moment and axial load on the cross section increased per the nonlinear soil-spring properties included in the model. In some cases, the analysis results indicated a high demand on the structure, which in turn required a significant increase in the diameter of the pile, concrete compressive strength, rebar yield strength and percentage of rebar. However, increasing these parameters resulted in an increase in the demand on the structure, sometimes at even a higher rate. This made it impractical to complete the design using a traditional deterministic approach per the provisions in design standards.

In the next series of analysis, bending moment plastic hinges were introduced in the model at the location of the maximum moment shown earlier in Figure 1. These bending moment plastic hinges were associated with the maximum bending moment capacity of the cross section, along with a zero shear demand, as illustrated earlier in Figure 4. For examples, for the cross section shown earlier in Figure 2 with 1% of longitudinal steel rebar, a plastic bending moment capacity of 5,130 kN-m was introduced in the model, which created a plateau on the maximum bending moment generated in the structure. Once the moment reached this maximum value, it stayed unchanged, which in turn resulted in significant decrease in the overall demand on the structure, including shear forces. Upon completion of the analysis, the shear demand was calculated, which was lower than the shear generated in the structure in cases where there was no limit imposed on the maximum bending moment capacity. However, the combination of the bending moment and shear demand (from the analysis output) were outside the interaction curve, meaning that the member was not able to resists the combined load. This combination of shear and bending moment demand were then compared against the interaction curves, and the plastic hinge maximum bending moment capacity was adjusted for the next round of analysis based on the interaction curve limits (see Figure 4). The analysis was repeated again and the resulting shear and bending moment demand were compared

against the analysis inputs. This procedure was repeated until the analysis outputs were very close to the analysis input, which indicated that the soil-structure interaction analysis had converged using a full coupled nonlinear analysis and design based on the principals of the MCFT.

As an example, Table 2 shows the results of a typical analysis performed in this study for a cross section with 1% of longitudinal reinforcement. The first analysis assumed a plastic hinge bending moment capacity of 5,130 (kN-m), along with a shear force of zero (See Figure 4). The analysis results, however, indicated a shear demand of 951 kN, which was outside the interaction curve shown in Figure 4 for a bending moment capacity of 5,130 (kN-m). In the next series of analysis, the plastic hinge maximum moment capacity was adjusted to 4,035 kN-m, which corresponds to a shear demand of 951 kN based on the interaction curve. After the completion of this analysis, the outputs were then used to revise the analysis input, and the analysis was repeated until convergence was achieved after six iterations. As observed in this table, the bending moment demand decreases from 5,130 (kN-m) to 4,298 (kN-m), while the shear demand simultaneously decreases from 951 (kN) to 869 (kN). This indicates a reduction of about 16% in the overall demand of the structure. In some analysis completed in this study, a reduction of up to 19% was observed for the overall demand on the structure. This is very valuable for cases when increasing the strength of the structure results in an even higher increase in the soil loads applied to the structure under large ground movements and liquefaction.

Table 2. Typical Results of the Iterative Procedure Used for Nonlinear Coupled Soil-Structure Interaction Analysis and Design

Iteration	Bending Moment (kN-m)	Shear (kN)
1	5,130	951
2	4,035	775
3	4,485	921
4	4,147	831
5	4,349	858
6	4,298	869

5 SUMMARY AND CONCLUTION

There exist many approaches for soil-structure interaction analysis of piles and shafts embedded in soil. However, these approaches do not take into consideration the real behavior of the structure and its complex interaction with soil. This study highlighted the importance of studying this coupled system in more detail, especially under soils liquefaction and large displacements, where both the soil and the structure enter the nonlinear range of the material response.

As observed in this study, when the soil forces applied to the structure increase and exceed a certain limit, the interactions between axial, moment, shear and torsional stresses become quite complex. This interaction not only influences how the structure behaves under the applied soil loads, but also changes the fundamental assumptions used for the soil-structure interaction analysis of this coupled system. The uncertainty in the response that comes with the implementation of simplified approaches leads to a conservative design, which is not cost-effective.

This study showed that the response of the structure and its ultimate load-carrying capacity changes quite abruptly for higher levels of stresses, especially when a plastic hinge is generated in the structure. The moment plastic hinge changes the overall response of the structure, which in turn changes the soil-loads. The soil-structure interaction analysis can be influenced by many other factors that are generally not captured using traditional design approaches. This includes various parameters such as brittle shear failure, fluctuation of axial forces and torsional stresses. This explains why a comprehensive soil-structure interaction analysis needs to consider both the nonlinear interaction between the soil and structure, as well as nonlinear behavior of the structure itself, along with its influence on the coupled system. In many cases, the generation of a plastic hinge moment puts a maximum limit on the forces that can be generated in the structure from soil, which in turn reduces the overall demand. This level of control on the behavior of this coupled system gives the engineer the ability to design the system to the requirements specified by the owner.

The nonlinear interaction mechanism between the soil and the structure can also consider other factors, which are currently under study by the author. This includes the depth of various soil layers, the diameter of the pile and shaft, and the length of the hinge zone.

6 REFERENCES

ASCE-ACI Committee 445, 1998. *Recent Approaches to Shear Design of Structural Concrete*, ASCE, Journal of Structural Engineering, Vol. 124, No. 12, pp. 1375-1417.

Belarbi, A. and Hsu, T. T. C. 1995. Constitutive Laws of Reinforced Concrete in Biaxial Tension-Compression, *Research Report UHCEE 91-2*, Department of Civil and Environmental Engineering, University of Houston, Houston, Texas: 155-162.

Bentz, E.C., Vecchio, F.J. and Collins, M.P. 2006. Simplified Modified Compression Field Theory for Calculating Shear Strength of Reinforced Concrete Elements, *ACI Structural Journal*, July-August: 614-624.

Bentz, E.C. and Collins, M.P. 2001. *User Manual – Response 2000*. University Of Toronto, Ontario, Canada.

Bentz, E.C. 2000. *Sectional Analysis of Reinforced Concrete*, Ph.D. Dissertation, Department of Civil Engineering, University of Toronto, Ontario, Canada.

Besseling, F. 2012. *Soil-structure Interaction Modelling in Performance-based Seismic Jetty Design*, M.Sc. Graduation Project, Delft University of Technology, Delft, Netherlands.

Cassese, P., De Risi, M. T. and Verderame, G. M. 2018. Seismic Assessment of Existing Hollow Circular Reinforced Concrete Bridge Piers, *Journal of Earthquake Engineering*, May.

Chai Y.H. and Hutchinson T.C. 2002. Flexural Strength and Ductility of Extended Pile-shafts. ii: Experimental Study, *Journal of Structural Engineering*, Vol. 128 (No. 5): 595–602.

Chandrakanth, B. and Whittaker, A. 2015. *Site Response, Soil-Structure Interaction and Structure-Soil-Structure Interaction for Performance Assessment of Buildings and Nuclear Structures*, Multidisciplinary Center for Earthquake Engineering Research, MCEER 15-0002.

Chun, B. and Shin, Y. 2006. Active earth pressure acting on the cylindrical retaining wall of a shaft, *South Korea Ground Environmental Engineering Journal*, 7(4): 15–24.

Collins, M. P., Bentz, E. C., Sherwood E. G. and Xie L. 2007. An Adequate Theory for The Shear Strength Of Reinforced Concrete Structures, Morley Symposium on Concrete Plasticity and its Application. University of Cambridge, July, 2007

Fujii, T. Hagiwara, T. Ueno, K. and Taguchi, A. 1994. Experiment and Analysis of Earth Pressure on an Axisymmetric Shaft in Sand, *Proceedings of 1994 International Conference on Centrifuge*, Balkema Rotterdam, Netherlands: 791–796.

Herten, M. and Pulsfort, M. 1999. Determination of Spatial Earth Pressure on Circular Shaft Constructions, *Granular Matter*, 2(1): 1–7.

Hsu, T. T. C. 1993. *Unified Theory of Reinforced Concrete*, CRC Press Inc. Boca Raton.

Hsu, T. T. C and Zhang, L-X. 1997. Nonlinear Analysis of Membrane Elements by Fixed-Angle Softened-Truss Model, *ACI Structural Journal*, 94(5): pp 483-492.

Iranpour, M. S. 1999. *A Study of Code-based Limit State Analysis Methods and P-Delta Secondary Effects in Simple Concrete Frames*, M.Sc. Dissertation, Shiraz University, Shiraz, Iran.

Konig, D. Guettler, U. and Jessberger, H.L. 1991. Stress Redistributions during Tunnel and Shaft Constructions, *Proceedings of the International Conference on Centrifuge*, Balkema Rotterdam, Netherlands: 129–135.

Krawinkler, H., Yang, T., Moehle, J. P., Bozorgnia, Y., Zareian, F., Wallace, J. W. 2012, Performance Assessment of Tall Concrete Core-Wall Building Designed Using Two Alternative Approaches, *Earthquake Engineering & Structural Dynamics,* 41(11): Sept. 2012

Kramer, S. L. Arduino, P. and Shin, H. 2008. *Using OpenSees for Performance-Based Evaluation of Bridges on Liquefiable Soils*, Pacific Earthquake Engineering Research Center, PEER 2008/07.

Lade, P. V. Jessberger, H.L., Makowski, E. and Jordan P. 1981. Modeling of Deep Shafts in Centrifuge Test, *Proceedings of International Conference on Soil Mechanics and Foundation Engineering*, Stockholm, Sweden, (1): 683–691.

Lam, I. P. Kapuskar, M. and Chaudhuri, D. 1998. *Modeling of Pile Footings and Drilled Shafts for Seismic Design*, Multidisciplinary Center for Earthquake Engineering Research, Technical Report MCEER-98-0018.

Matlock, H. 1970. Correlation for Design of Laterally Loaded Piles in Soft Clay, *2nd Annual Offshore Technology Conference*, Houston, Texas

Miranda, E. 2014. Lessons Learned from the 2010 Haiti Earthquake for Performance-Based Design. *Performance-Based Seismic Engineering: Vision for an Earthquake Resilient Society*: 117-127

Pang, X.B. and Hsu, T. T. C. 1996. Fixed Angle Softened Truss Model for Reinforced Concrete, *ACI Structural Journal*, 93(2): 197-207.

Qian, K. Li, B. & Liu, Y. 2017. Experimental and Analytical Study on Load Paths of RC Squat Walls with Openings. *Magazine of Concrete Research*, 69(1): 1-23.

Reese, L. Cox, W. and Koop, R. 1974. Analysis of Laterally Load Piles in Sand, 6th Annual Offshore Technology Conference, Paper No. 2080

Rollins K. M., Gerber, T.M. Lane D. and Ashford S. A. 2005. Lateral Resistance of a Full-scale Pile Group in Liquefied Sand. Journal of *Geotechnical and Geoenvironmental Engineering*, ASCE, 131(1): 115–125.

Tobar, T. and Meguid, M. A. 2010. Comparative Evaluation of Methods to Determine the Earth Pressure Distribution on Cylindrical Shafts: A review. *Tunnelling Underground Space Technol*. 25(2): 188–197.

Tobar, T. and Meguid, M. A. 2011. Experimental Study of the Earth Pressure Distribution on Cylindrical Shafts, *Journal of Geotechnical and Geoenvironmental Engineering*, Nov., 1121-1125

Tokimatsu K. Suzuki H. and Suzuki Y. 2001. Back-calculated p-y Relation of Liquefied Soils from Large Shaking Table Tests. *Fourth International Conference on Recent Advances in Geotechnical Earthquake Engineering and Soil Dynamics*, (Paper No. 6.24): 672–690.

Vecchio, F.J. and Collins, M.P. 1986. The Modified Compression Field Theory for Reinforced Concrete Elements Subjected to Shear", *ACI Journal*, Proceedings 83(2): 219-231.

Walz, B. 1973. Left Bracket Apparatus for Measuring the Three Dimensional Active Soil Pressure on a Round Model Caisson Right Bracket. Baumaschine und Bautechnik, 20(9): 339-344.

Weaver T. J. Ashford S.A. and Rollins K. M. 2005. Response of 0.6 m Cast-in-steel-shell Pile in Liquefied Soil under Lateral Loading. *Journal of Geotechnical and Geoenvironmental Engineering*, ASCE, Vol. 131(1): 94-102.

Wilson D. W. Boulanger R. W. and Kutter B. L. 2000. Observed Seismic Lateral Resistance of Liquefying Sand. *Journal of Geotechnical and Geoenvironmental Engineering*, ASCE, 126(10): 898-906.

Zhang, L-X and Hsu, T. T. C. 1998. Behavior and Analysis of 100 MPa Concrete Membrane Elements, Journal of Structural Engineering, ASCE, 124(1): pp 24-34